AEDC-TR-75-118

CALCULATION OF THE BOUNDARY-LAYER GROWTH IN A LUDWIEG TUBE

VON KÁRMÁN GAS DYNAMICS FACILITY
ARNOLD ENGINEERING DEVELOPMENT CENTER
AIR FORCE SYSTEMS COMMAND
ARNOLD AIR FORCE STATION, TENNESSEE 37389

December 1975

Final Report for Period July 1973 – December 1974

Prepared for

DIRECTORATE OF TECHNOLOGY (DY)
ARNOLD ENGINEERING DEVELOPMENT CENTER
ARNOLD AIR FORCE STATION, TENNESSEE 37389

NOTICES

When U. S. Government drawings specifications, or other data are used for any purpose other than a definitely related Government procurement operation, the Government thereby incurs no responsibility nor any obligation whatsoever, and the fact that the Government may have formulated, furnished, or in any way supplied the said drawings, specifications, or other data, is not to be regarded by implication or otherwise, or in any manner licensing the holder or any other person or corporation, or conveying any rights or permission to manufacture, use, or sell any patented invention that may in any way be related thereto.

Qualified users may obtain copies of this report from the Defense Documentation Center.

References to named commercial products in this report are not to be considered in any sense as an endorsement of the product by the United States Air Force or the Government.

This report has been reviewed by the Information Office (OI) and is releasable to the National Technical Information Service (NTIS). At NTIS, it will be available to the general public, including foreign nations.

APPROVAL STATEMENT

This technical report has been reviewed and is approved for publication.

FOR THE COMMANDER

Carlos Tirres

CARLOS TIRRES
Captain, USAF
Research & Development
Division
Directorate of Technology

Robert O Dietz

ROBERT O. DIETZ
Director of Technology

REPORT DOCUMENTATION PAGE		READ INSTRUCTIONS BEFORE COMPLETING FORM
1 REPORT NUMBER AEDC-TR-75-118	2 GOVT ACCESSION NO	3 RECIPIENT'S CATALOG NUMBER
4 TITLE (and Subtitle) CALCULATION OF THE BOUNDARY-LAYER GROWTH IN A LUDWIEG TUBE		5 TYPE OF REPORT & PERIOD COVERED Final Report-July 1973 - December 1974 6 PERFORMING ORG. REPORT NUMBER
7 AUTHOR(s) James C. Sivells, ARO, Inc.		8 CONTRACT OR GRANT NUMBER(s)
9 PERFORMING ORGANIZATION NAME AND ADDRESS Arnold Engineering Development Center (DY) Arnold Air Force Station, Tennessee 37389		10 PROGRAM ELEMENT, PROJECT, TASK AREA & WORK UNIT NUMBERS Program Element 65807F
11 CONTROLLING OFFICE NAME AND ADDRESS Arnold Engineering Development Center (DYFS) Arnold Air Force Station, Tennessee 37389		12 REPORT DATE December 1975 13 NUMBER OF PAGES 36
14 MONITORING AGENCY NAME & ADDRESS (if different from Controlling Office)		15 SECURITY CLASS. (of this report) UNCLASSIFIED 15a DECLASSIFICATION DOWNGRADING SCHEDULE N/A

16 DISTRIBUTION STATEMENT (of this Report)

Approved for public release; distribution unlimited.

17 DISTRIBUTION STATEMENT (of the abstract entered in Block 20, if different from Report)

18 SUPPLEMENTARY NOTES

Available in DDC

19 KEY WORDS (Continue on reverse side if necessary and identify by block number)

computations	Ludwieg tube	expansion
boundary layer	transonic flow	wave
growth	wind tunnels (pilot)	
measurement	Reynolds number	

20 ABSTRACT (Continue on reverse side if necessary and identify by block number)

Experimental boundary-layer measurements obtained in a Ludwieg tube used to drive a pilot transonic tunnel were compared with values calculated by a procedure developed by E. Becker and with those calculated by a method containing several modifications to Becker's method. The modifications fall into three general categories: the use of a skin-friction law and velocity profile exponent which are more accurate at high Reynolds numbers;

DD FORM 1 JAN 73 1473 EDITION OF 1 NOV 65 IS OBSOLETE

20. ABSTRACT (Continued)

treatment of the momentum equation as axisymmetric instead of two-dimensional; and calculation at a specified location other than at the origin of the centered expansion wave. Inasmuch as these modifications greatly improved the agreement with experimental values, they are presented herein.

CONTENTS

ILLUSTRATIONS

APPENDIX

1.0 INTRODUCTION

In a wind tunnel driven by a Ludwieg tube (Ref. 1), the air in the wind tunnel and tube is initially compressed to a desired charge pressure. Flow is initiated by breaking a diaphragm, or quickly opening a valve, located downstream of the test section. As the air is released, an expansion wave is created and travels upstream to the closed end of the tube where it is reflected and returned to the contraction section at the downstream end. Due to viscous effects in the airflow generated by the expansion wave, a boundary layer is formed whose thickness increases with time. During this excursion of the expansion wave, the stagnation pressure of the central core of flow through the wind tunnel is essentially constant until the thickness of the boundary layer at the downstream end of the tube approaches the radius of the tube. Thus, the useful run time for the Ludwieg tube wind tunnel depends upon the initial air temperature which determines the velocity of the head of the expansion wave, the length of the tube which is traversed by the expansion wave, and the diameter of the tube which determines the velocity of the airflow and relative to which the boundary-layer thickness eventually becomes critical.

Shortly after the conception of the tube wind tunnel, calculations of the growth of the boundary layer were made by E. Becker, (Refs. 2 and 3). Values calculated by Becker's method, however, considerably underestimated the boundary-layer thicknesses obtained experimentally in a pilot tunnel as shown in Fig. 1, which was presented in

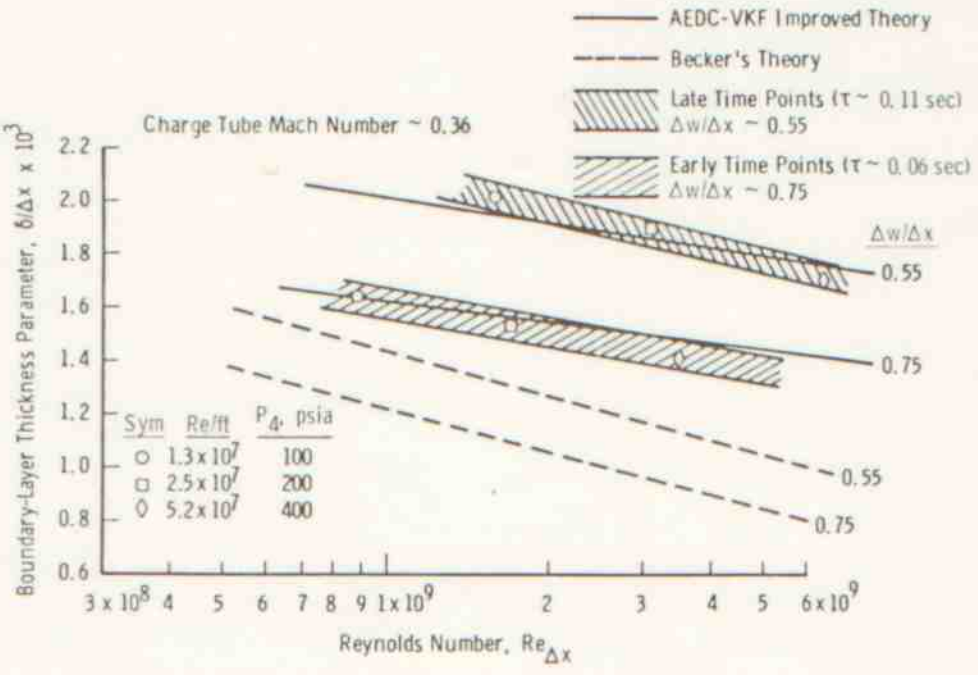

Figure 1. Charge tube boundary-layer thickness.

Ref. 4. In this figure, the Reynolds number is based on the distance Δx between the head of the expansion wave and the measuring station. Data are presented for two times, when the length of the expansion wave ΔW (head to tail) was about 55 and also about 75 percent of Δx. Three values of charge pressure P_4 are indicated.

Scrutiny of Becker's procedure indicated three categories in which modifications could be made to improve its correlation with the experimental data: the use of a skin-friction law and boundary-layer velocity-distribution which are more accurate at high Reynolds number; treatment of the momentum equation as axisymmetric instead of two-dimensional; and calculation at a specified location other than at the origin of the centered expansion wave. The latter is particularly important for a transonic wind tunnel utilizing a plenum chamber surrounding a porous-wall test section because the establishment of steady-state conditions in the test section determines when the tail of the expansion wave starts upstream through the Ludwieg tube.

When Becker's procedure was so modified, the results indicated as the AEDC-VKF improved method in Fig. 1 were obtained. The improvement in correlation with data from the pilot tunnel was considered to be sufficient to warrant the use of the modified method in any future applications.

2.0 THEORY OF OPERATION

The principle of operation can be described with the help of the wave diagram of Fig. 2. This diagram differs from the usual diagram which considers the diaphragm to be located at the downstream end of the tube. In the practical case of a transonic wind tunnel. the diaphragm or start valve is located downstream of the test section. When flow is initiated, the expansion wave travels upstream. The velocity of the head of the wave is the speed of sound a_o at the temperature of the charge air. The velocity of the air leaving the tube u_1 is determined by the ratio of the tube area to the area where the flow is sonic.

$$\frac{A_{tube}}{A^*} = \frac{1}{M_1}\left(\frac{2}{\gamma+1} + \frac{\gamma-1}{\gamma+1} M_1^2\right)^{\frac{\gamma+1}{2(\gamma-1)}} \tag{1}$$

and

$$M_1 = u_1/a_1 \tag{2}$$

The velocity of sound, a_1, in the air, after the flow is established, is related to a_o.

$$a_1/a_o = 1\Big/\left(1 + \frac{\gamma-1}{2} M_1\right) \tag{3}$$

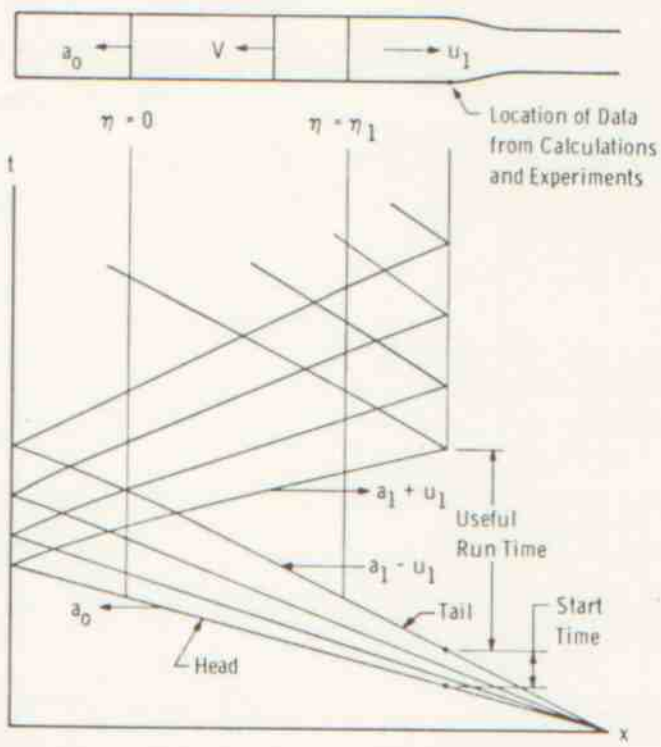

Figure 2. Characteristic diagram of expansion wave.

The velocity of the tail of the wave is $a_1 - u_1$; thus, the length of the expansion wave increases with time. The wave length is approximately linear with time after the wave is completely in the charge tube. For simplicity, it is also shown in Fig. 2 as linear downstream of the charge tube by extending the lines denoting the head and the tail of the wave until they meet at an effective location of the origin of the expansion wave. In the actual case of a porous-wall transonic test section, some time is spent in establishing steady-state conditions in the test section and plenum chamber. This in turn produces a noncentered wave process in the charge tube. The start time indicated in Fig. 2 is defined as the period of time during which the pressure at the end of the charge tube decreases from its charge value P_4 to the value of P_1 following the passage of the tail of wave, where

$$P_1/P_4 = (a_1/a_o)\frac{2\gamma}{\gamma - 1} \tag{4}$$

From a knowledge of the start time, either from measurement or estimate, the effective time and position at which the wave length is zero can be determined.

In the development of the boundary-layer calculation, Becker solved the momentum equation twice: once for the growth of the boundary layer within the expansion wave

and again for the growth of the boundary layer behind a fictitious concentrated wave of zero length moving at a velocity V intermediate between the velocities at the head and tail of the actual expansion wave. The value of this velocity was found by finding the distance behind the fictitious wave at which the boundary-layer thickness was the same as that at the tail of the expansion wave from the first solution. Becker introduced the variable η, where

$$\eta = 1 - \frac{x}{a_o t} \tag{5}$$

and η varies from 0 at the head of the expansion wave to η_1 at the tail and

$$\eta_1 = \frac{\gamma + 1}{2} \; M_1 \Big/ \left(1 + \frac{\gamma - 1}{2} \; M_1\right) \tag{6}$$

When Becker matched his boundary-layer solutions, he obtained a relation between V and u_1 (or a_o). When his relationship is expressed in a series on powers of η_1, it can be shown that

$$V/a_o = 1 - 2\eta_1/3 \tag{7}$$

is sufficiently accurate for practical values of η_1 up to about 0.45 and is independent of the choice of velocity profile exponent and friction coefficient law since these are contained only in the negligibly small coefficients of η_1^2 and higher powers of η_1. In the subsequent development of the modifications to improve the correlation of theory with experiment, it is assumed that this relationship, Eq. (7), is accurate inasmuch as only the flow behind the fictitious concentrated wave is considered.

3.0 MOMENTUM EQUATION

The time-dependent momentum equations for internal tube flow is adapted from Ref. 5 as

$$u_1 \frac{\partial}{\partial t} \int_0^{\delta} \left(1 - \frac{y}{r}\right) (\rho - \rho_1) \, dy + \frac{\partial}{\partial t} (\rho_1 u_1 \delta_1) + \frac{\partial u_1}{\partial y} \rho_1 u_1 \delta_1 + \frac{\partial}{\partial y} (\rho_1 u_1^2 \theta_1) = \tau_w \tag{8}$$

$$\delta_1 = \int_0^{\delta} \left(1 - \frac{y}{r}\right) \left(1 - \frac{\rho u}{\rho_1 u_1}\right) dy \tag{9}$$

$$\theta_1 = \int_0^{\delta} \left(1 - \frac{y}{r}\right) \frac{\rho u}{\rho_1 u_1} \left(1 - \frac{u}{u_1}\right) dy \tag{10}$$

$$\delta_1 = \delta^* - \delta^{*2}/2r \tag{11}$$

$$\theta_1 = \theta - \theta^2/2r \tag{12}$$

The quantities, δ_1 and θ_1, may be considered to be the displacement and momentum thicknesses when the boundary-layer thickness is small with respect to the radius of the tube. When the boundary-layer thickness is not small relative to the radius, the true values of δ^* and θ, obtained from mass-defect and momentum-defect considerations must be used to assess their effects on the flow but δ_1 and θ_1 are still used in Eq. (8). Becker did not use the (1 - y/r) term in Eq. (8), (9), or (10), in which case Eq. (8) reduces to the two-dimensional form. In Ref. 1, Becker omitted the first term of Eq. (8). In Ref. 2, he included this term and also included the effects of compressibility and heat transfer on the ratio of ρ/ρ_1 within the boundary layer and upon the friction coefficient, and obtained essentially the same result (within about one percent) as for the incompressible case, at least for the usual conditions of operation of a Ludwieg tube.

The momentum equation can be simplified if it is assumed that the free-stream values of u_1 and ρ_1 are independent of time and a definition is added

$$\rho^* = \int_0^{\delta} \left(1 - \frac{y}{r}\right)\left(\frac{\rho}{\rho_1} - 1\right) dy \tag{13}$$

Also, in Eq. (8) the direction of x is positive in the direction u_1, but for the present purpose x is positive in the direction of wave propagation. Then

$$\frac{1}{u_1}\frac{\partial}{\partial t}(\rho^* + \delta_1) - \frac{\partial \theta_1}{\partial x} = \frac{\tau_w}{P_1 u_1^2} = \frac{C_f}{2} \tag{14}$$

It is assumed that the ratio $(\rho^* + \delta_1)/\theta_1$ is relatively independent of time. Then

$$\frac{\rho^* + \delta_1}{\theta_1 u_1}\frac{\partial \theta_1}{\partial t} - \frac{\partial \theta_1}{\partial x} = \frac{C_f}{2} \tag{15}$$

This equation can be integrated through the introduction of the distance $\overline{X}$ defined as

$$\overline{X} = Vt - x \tag{16}$$

which is the distance from the concentrated wave to the point x, and x and t are zero at the effective origin of the expansion wave. It is further assumed that the friction coefficient is a function of equivalent flat-plate momentum thickness, θ_c, such that

$$C_f/2 = d\theta_c/d\overline{X} \tag{17}$$

In the absence of a longitudinal pressure gradient, Eq. (17) can be integrated to give

$$C_F/2 = \theta_c/\overline{X} \tag{18}$$

where the constant of integration is neglected. Eq. (15) can thus be integrated to give

$$\left(\frac{V}{u_1}\,\frac{\rho^* + \delta_1}{\theta_1} + 1\right)\theta_1 = \theta_c = \overline{X}\,C_F/2 = (Vt - x)\,C_F/2 \tag{19}$$

After rearranging

$$\theta_1 = \frac{(Vt - x)\,C_F/2}{1 + \frac{V}{u_1}\,\frac{\rho^* + \delta_1}{\theta_1}} \tag{20}$$

Finally,

$$\delta = \frac{\delta}{\theta_1}\,\frac{(Vt - x)}{1 + \frac{V}{u_1}\,\frac{\rho^* + \delta_1}{\theta_1}} \tag{21}$$

The ratios, δ/θ_1, ρ^*/θ_1, δ_1/θ_1, are obtained from Eqs. (9), (10), and (13) after the velocity and density distributions are assumed and

$$V/u_1 = (1/M_1) - (5 - \gamma)/6 \tag{22}$$

from Eqs. (2), (3), (6) and (7). The friction coefficient must be in a form which can be integrated with respect to the momentum thickness and must be corrected for at least first-order effects of compressibility and heat transfer. The heat transfer is from the wall to the air inasmuch as the mass of the wall is considered to be sufficient that its temperature is essentially constant during the short run time.

Except for the definition of the various parameters, the above derivation follows that of Becker. When x = Vt, i.e. at the location of the concentrated wave, the boundary-layer thickness is zero and increases, for a given value of t, as x decreases to zero. In the present treatment, the lowest value of t to be considered is the time required for the tail of the expansion wave to reach the downstream end of the charge tube and the value of x is the effective distance traveled by the wave tail. In Becker's evaluation of the boundary-layer parameters, he assumed that

$$u/u_1 = (y/\delta)^{1/7} \tag{23}$$

$$\frac{\rho - \rho_w}{\rho_1 - \rho_w} = \frac{u}{u_1} \tag{24}$$

$$C_{f_i} = 0.045\ Re_\delta^{-1/4} \tag{25}$$

and

$$C_{f_i}/C_f = F_c = \left(\frac{T_w + T_1}{2T_1}\right)^{1/2} \tag{26}$$

The accuracy of this choice of parameters is optimum for values of Re_δ of about 100,000 but deteriorates as the Reynolds number increases.

4.0 SKIN-FRICTION COEFFICIENT

One widely used expression for incompressible skin friction which correlates well with experimental data over a wide range of Reynolds numbers is that of von Kármán and Schoenherr (Ref. 6)

$$C_{f_i} = \frac{(0.242)^2}{(log\ Re_{\theta_i} + 1.1696)\,(log\ Re_{\theta_i} + 0.3010)} \tag{27}$$

which can be integrated to give the familiar

$$C_{f_i}^{1/2} = 0.242/log\,(2\ Re_{\theta_i}) \tag{28}$$

Another expression (Ref. 7) is that based on Coles' law of the wall and law of the wake

$$\kappa\ (2/C_{f_i})^{1/2} = \ell n\ Re_\delta + 0.5\ \ell n\ (C_{f_i}/2) + \kappa C + 2\Pi \tag{29}$$

where the constants κ and C are 0.41 and 5.0, respectively, and Π is a function of Reynolds number and pressure gradient. If the laminar sublayer is neglected and the wake function is represented by a $\sin^2$ distribution, integration of the profile gives

$$\frac{\delta_i^*}{\delta} = \frac{1 + \Pi}{\kappa}\left(\frac{C_{f_i}}{2}\right)^{1/2} \tag{30}$$

and

$$\frac{\theta_i}{\delta} = \frac{\delta_i^*}{\delta} - \frac{C_{f_i}}{2\kappa^2}\,(2 + 3.179\ \Pi + 1.5\ \Pi^2) \tag{31}$$

Equations (30) and (31) must be used with Eq. (29) to determine C_{f_i} as a function of Re_{θ_i}. It may be noted that for an earlier version of the wake distribution (Ref. 8), the coefficients of Π and Π^2 in Eq. (31) were 3.2 and 1.522, respectively.

In order to use Eq. (29), values of Π must be known as a function of Reynolds number, even for the zero pressure gradient condition assumed herein. For the wake distribution used in Ref. 8, Coles found that Π seemed to have a constant value of 0.55 for values of Re_{θ_i} greater than about 6,000. For the sine^2 distribution used to obtain Eq. (31), the value of Π must be increased slightly to about 0.56 at $Re_{\theta_i} = 5{,}000$ and further to about 0.58 at $Re_{\theta_i} = 29{,}000$ in order to match the tabulated values of C_{f_i} therein. Even if Eq. (29) could be put into a form which could be integrated, the question arises as to how Π varies with Reynolds number to values about three orders of magnitude higher than that considered by Coles. Such large Reynolds numbers would be encountered in a large Ludwieg tube. Even the high Reynolds numbers of the experimental values of Kempf (Ref. 9) are about two orders of magnitude too low for comparison with a large Ludwieg tube.

If it is assumed that both Eqs. (27) and (29) give identical results and Eq. (31) is used to relate Re_{θ_i} with Re_δ, values of Π can be calculated by an iterative method. The results are shown in Fig. 3 and indicate an increasing value of Π with increasing Reynolds number.

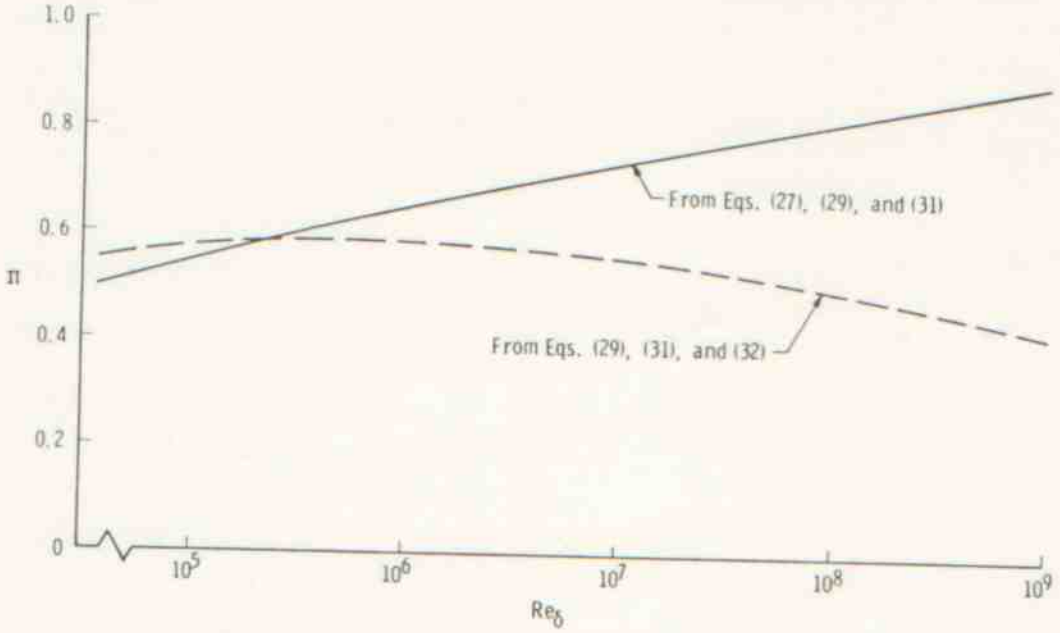

Figure 3. Variation of Π with Reynolds number.

A third expression for skin-friction coefficient used in Ref. 10* is

$$C_{f_i} = \frac{0.0773}{(log\ Re_{\theta_i} + 4.561)\,(log\ Re_{\theta_i} - 0.546)} \qquad (32)$$

*Constant 4.561 in Eq. (32) was 4.563 in Eq. (70) of Ref. 10.